PREPARED FOR
ELECTRIC RELIABILITY COUNCIL OF TEXAS (ERCOT)

Solar Site Screening and Hourly Generation Profiles

Ref. No.: 03-16-014484

January 31, 2017

CLASSIFICATION

FOR PUBLIC RELEASE

ISSUE

B

KEY TO DOCUMENT CLASSIFICATION

STRICTLY CONFIDENTIAL	For recipients only
CONFIDENTIAL	May be shared within client's organization
AWS TRUEPOWER ONLY	Not to be distributed outside AWS Truepower
CLIENT'S DISCRETION	Distribution at the client's discretion
FOR PUBLIC RELEASE	No restriction

DOCUMENT CONTRIBUTORS

AUTHOR(S)	REVIEWER(S)	APPROVED BY
Rojowsky, Katherine	Frank, Jaclyn	Shakarjian, Mikel

DOCUMENT HISTORY

Issue	Date	Summary
A	12/19/2016	Draft
B	1/31/2017	Final

TABLE OF CONTENTS

LIST OF FIGURES

LIST OF TABLES

1. INTRODUCTION

On behalf of the Electric Reliability Council of Texas (ERCOT), AWS Truepower (AWST), a UL Company, developed hourly solar generation profiles for 1997-2015 and performed a site screening study for both utility-scale solar photovoltaic (PV) plants and distributed solar PV resources (DPV) across the state of Texas. AWST estimated the potential DPV for the greater urban areas of Austin, Dallas, Houston and San Antonio, based on land use classifications. AWST simulated hourly PV generation for these urban areas as well as for hypothetical and existing utility-scale PV sites. The hypothetical utility-scale sites were modeled with both single- and dual-axis configurations. Existing utility-scale sites were modeled to match plant configurations as closely as possible. DPV was modeled with fixed modules tilted 22.6 degrees (a common rooftop pitch in Texas) oriented south, southeast, and southwest. AWST created the hourly solar generation profiles using data from the Weather Research and Forecasting (WRF) model and power simulation from an AWST model. This report describes the methods, results, and validations for the site screening study and hourly power profile development.

2. MESOSCALE MODELING

Historical meteorological conditions were simulated over the project area with the Weather Research and Forecasting (WRF) model and leveraged work from previous modeling performed on behalf of ERCOT to support annual wind generation profiles.[1,2,3] WRF, a leading open-source community numerical weather prediction (NWP) model, was used to generate the historical atmospheric variables such as wind speed, temperature and irradiance, necessary to simulate solar power production at each location.[4] WRF simulates the fundamental physics of the atmosphere, including conservation of mass, momentum, energy, and the moisture phases (water vapor, cloud, ice, rain, and snow), using a variety of online, global geophysical and meteorological databases. The atmospheric variables were computed and adjusted using surface station data and then stored as input to AWST's proprietary model to produce the hourly power simulations. For these studies, a nested grid scheme with horizontal resolutions of 27 kilometers (km) and 9 km was used. Details of the model configuration can be found in AWST (March 2015). Hourly global horizontal, direct normal, and diffuse horizontal irradiance; 2-meter (m) temperature; 10-m wind speed; and precipitation values were extracted from the 9-km resolution model runs for the period 1997-2015.

---

[1] AWS Truepower, LLC, "Simulation of Wind Generation Patterns for the ERCOT Service Area", Report to ERCOT, March 2015.

[2] AWS Truepower, LLC, "Simulated Wind Generation Profiles 2014", Report to ERCOT, July 2015

[3] AWS Truepower, LLC, "Simulated Wind Generation Profiles 2015", Report to ERCOT, June 2016

[4] http://www.wrf-model.org/index.php

3. SOLAR RESOURCE MAP

The solar resource was defined using a map of the average annual global horizontal solar irradiance (GHI) previously developed by AWST at a spatial resolution of 10-km. This map was downscaled to 200-m and the resulting high-resolution map was used to complete the solar site screening.

The 10-km GHI map was created using the Mesoscale Atmospheric Simulation System (MASS), a dynamical weather model developed by AWS Truepower.[5] This map had been constructed from 15 years of atmospheric simulations, adjusted to surface data, and represents the long-term average irradiance.

AWST applied the Geographic Resources Analysis Support System (GRASS) software[6] r.sun solar radiation model to adjust the 10-km resolution irradiance dataset to yield a high resolution, 200-m irradiance map. The adjustment accounted for the effects of regional topography on local insolation values by using digital elevation model (DEM) data at both 10-km and 200-m resolution. Figure 3.1 and Figure 3.2 illustrate the downscaling for an area of complex terrain located in Jeff Davis County in western Texas. (High irradiance is depicted in dark orange/brown shades, lower irradiance in yellow and green.) The r.sun downscaling approach decreases global horizontal irradiance due to horizon shadowing based on the resolution of the input elevation data set. Areas of apparent irradiance increase are due to finer resolution elevation data where portions of a valley at 10 km may include a local ridge at 200 m and are not shadowed. This resolution is sufficiently fine to reflect the influence of most terrain features on irradiance and is useful for selecting ideally located utility-scale PV sites.

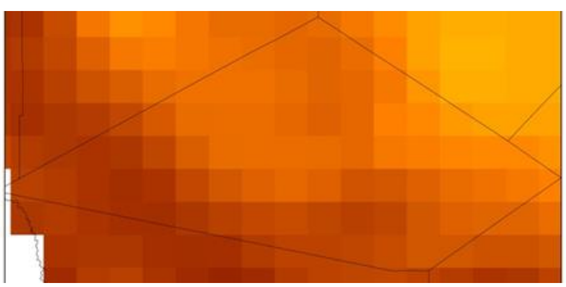

Figure 3.1: 10-km GHI in area of complex terrain before AWST downscaling

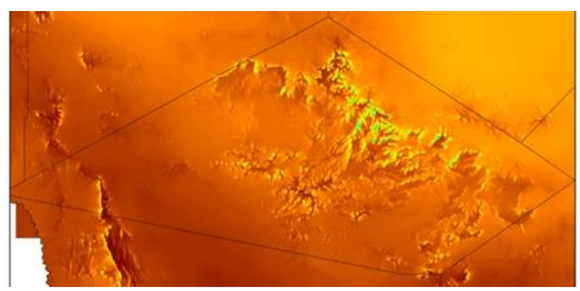

Figure 3.2: 200-m GHI in area of complex terrain after AWST downscaling

[5] Manobianco, J., J. W. Zack, and G.E. Taylor, 1996: Workstation-based real-time mesoscale modeling designed for weather support to operations at the Kennedy Space Center and Cape Canaveral Air Station. Bull. Amer. Meteor. Soc., 77, 653-672. Available online at http://science.ksc.nasa.gov/amu/journals/bams-1996.pdf.

[6] Geographic Resources Analysis Support System (GRASS) Software, Version 6.4.4. Open Source Geospatial Foundation. http://grass.osgeo.org

4. SITE SELECTION

The feasibility of a solar plant is driven by a complex relationship between the available solar resource at a proposed site and the ability to design, construct, and operate a plant at that location. Several important variables also play a role in the potential for development. They include, among others, existing land use, terrain slope, and protected status.

AWST used a Geographical Information System (GIS) based approach to identify development constraints and build out potential sites for utility-scale PV and DPV generation across the project areas of Texas. Although the ERCOT region does not include all of Texas, this approach allows for study of solar resources that are outside of the ERCOT boundaries but electrically connected to the ERCOT grid. In total, 6250 MW of utility-scale PV sites (125 plants at 50 MW each) were selected based on their solar irradiance and geographic distribution. Using available data in Texas as well as previous studies in other locations, it was determined that there was no appreciable difference between hourly ramps at 50-MW or 200-MW plants,[7] therefore the 50-MW profiles are scalable linearly up to 200 MW to total 25,000 MW of potential capacity. Four urban areas (Austin, Dallas, Houston, and San Antonio) were screened for DPV capacity, and results were provided by land use category for each greater urban area.

4.1 Utility-Scale PV Site Screening

4.1.1 Assumptions

AWST used an automated GIS-based site screening approach to identify sites for potential utility-scale solar PV projects. The land classifications considered for utility-scale PV development include shrub land, grassland or pasture, and cropland, as classified by the National Land Cover Database. Areas excluded from utility-scale PV development are comprised of AWST-standard assumptions as well as those specific to the ERCOT region to remove potential flood-prone areas (perennial/intermittent streams, coastal areas, special flood hazard areas). A complete listing of these can be found in Table 4.1.

Coastal and flash flooding was identified as a hazard in the project area, and additional exclusions were applied in vulnerable areas. The FEMA National Flood Hazard Layer[8] was obtained, and vulnerable areas were identified based on their assessment in the digital Flood Insurance Rate Map (dFIRM) database as Special Flood Hazard Areas, which would be covered by floodwaters of the base flood (1-percent annual chance), and where the National Flood Insurance Program regulations are enforced and flood insurance

[7] The leading edge of a cloud moving 10 m/s will take just over 4 minutes to pass diagonally across a 200-MW PV plant with a density of 60 MW_{AC}/km^2. Assuming an average cumulus cloud size of 1000 m, it takes an additional 2 minutes for the back edge of the cloud to cross the PV plant. Therefore the entire ramp lasts less than 10 minutes at a 200-MW plant, and less than half that time at a 50-MW plant. It follows that the variability should not be much different for a 50-MW versus a 200-MW plant on an hourly timescale.

[8] FEMA National Flood Hazard Layer (2015). Texas Natural Resources Information System. https://tnris.org/data-catalog/entry/fema-national-flood-hazard-layer/

is mandatory.[9,10] Because not all counties are included in this database, additional measures were taken to exclude other flood prone locations. Areas of elevation less than 5 m were excluded. The topography of Texas is such that these locations are found only within coastal locations, effectively eliminating the areas vulnerable to coastal flooding. Historical storm tide values from hurricanes with notable surge events were analyzed, and justified use of this 5-m threshold.[11] Inland streamflow flooding hazard was also mitigated by excluding areas within 1,000 feet of perennial streams and rivers or within 500 feet of intermittent streams.

Table 4.1: Exclusions and Setbacks for Utility-Scale Solar PV Site Screening

Data Layer	Exclusion Applied	Data Source
Land Cover	Open Water	National Land Cover Database 2011
	Developed Open Area Space/Urban Areas	
	Forested Areas	
	Wetlands (100-ft. buffer)	USFWS Wetland Database
Land Use	Conservation Easements	National Conservation Easement Database
	Parks & Non-Public Federal Lands	USGS Protected Area Database
	Protected Areas	
Waterbodies	Perennial streams (1000-ft. buffer)	ESRI data
	Intermittent streams (500-ft. buffer)	
Terrain	Areas which exceed 5% slope	National Elevation Dataset
	Areas with elevation less than 5 m (coastal)	
FEMA Flood Areas	Special Flood Hazard Areas: areas inundated by the base (1% annual chance) flood	FEMA National Flood Hazard Layer

4.1.2 Site Selection

The utility-scale solar PV site screening was completed using AWST's internal software application. The program operates in two main steps. In the first step, it finds all sites with a maximum irradiance in the immediate vicinity (i.e., a local maximum) with sufficient area to support a project of a desired size. For the ERCOT region, this target installed capacity was set to 50 MW, with an assumed site density of 60 MW_{AC}/km^2. In the second step, the program allows each of these sites to expand so long as the net capacity factor does not decrease by more than 5%. If the site encounters another site, the site that has a higher mean output is retained and the other is dropped. This process yielded over 6,000 sites distributed amongst all Texas counties.

[9] Special Flood Hazard Area. Federal Emergency Management Agency. https://www.fema.gov/special-flood-hazard-area

[10] How to Read a Flood Insurance Rate Map Tutorial. Federal Emergency Management Agency. https://www.fema.gov/media-library/assets/documents/7984

[11] Storm Surge Overview. National Hurricane Center. http://www.nhc.noaa.gov/surge/

In consultation with ERCOT, it was determined that the final sites selected would be located within the counties in the western part of the state, where the solar resource is highest in terms of mean annual GHI and utility-scale PV development is most likely. One additional profile would be located in each of the four counties that encompass the cities of Austin, Dallas, Houston, and San Antonio. To identify counties for which site profiles would be generated, the average annual irradiance for each county was evaluated (Figure 4.1). Counties in West Texas (where irradiance values are highest) would be represented by two time series generation profiles. Counties in central and southern Texas, as well as the Texas Panhandle, would be represented by one. The number of profiles provided for each county is indicated by the size of the black circles in Figure 4.1 (2 profiles provided for counties with a large circle, 1 profile for small circle counties).

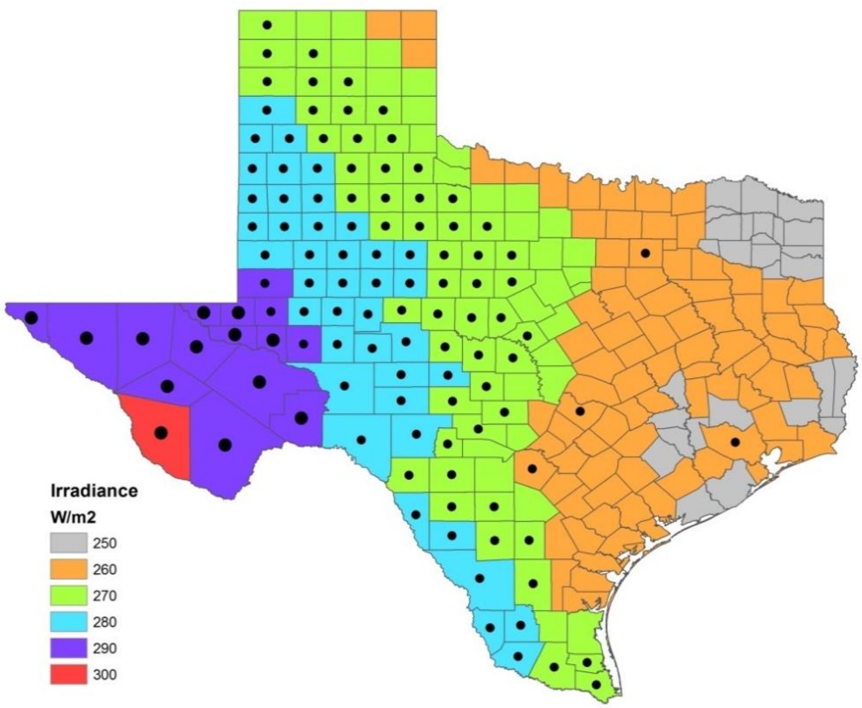

Figure 4.1: Average Global Horizontal Irradiance (GHI) by County in W/m^2

The output of the automated screening algorithm was further evaluated to determine site locations for hourly profile development. All counties with a marker as indicated in Figure 4.1 would receive one site profile based on the highest irradiance area within its boundary that is most conducive to utility-scale development. To identify the highest irradiance sites, the top 10 highest irradiance sites per county were manually screened using aerial imagery. Priority was given to the site(s) with the highest irradiance located on agricultural land, and active oil fields were avoided. Sites were iteratively selected to maximize distance between profiles (within and across counties). Selected site locations were optimized so that no two site centroids were within 20 km of one another. For counties where secondary sites would be provided, secondary sites were selected if their irradiance values equaled median values of their respective counties (so as to introduce diversity in the generation profiles and geographic distribution). A listing of counties for which profiles were developed, along with their individual site number(s), can be found in the Appendix.

4.2 Distributed PV Site Screening

4.2.1 Assumptions

AWST evaluated four urban areas (Austin, Dallas, Houston, and San Antonio) for DPV generation. Because densely populated areas were found outside the border of these cities, the greater urban areas of these cities were identified. The greater urban areas comprise of concentrated areas defined as low, medium, or high intensity development,[12] and include the 4 major cities, as well as their greater metropoleis (which may contain bordering cities, extraterritorial jurisdictions, enclaves, etc.). As an example, the greater urban area is colored grey in Figure 4.2, and the areas of low, medium, and high intensity development are green, yellow, and red, respectively. These three land use classes within each greater urban area delineate the area evaluated for DPV generation (the "metro region"). Developed areas outside of the greater urban areas were excluded.

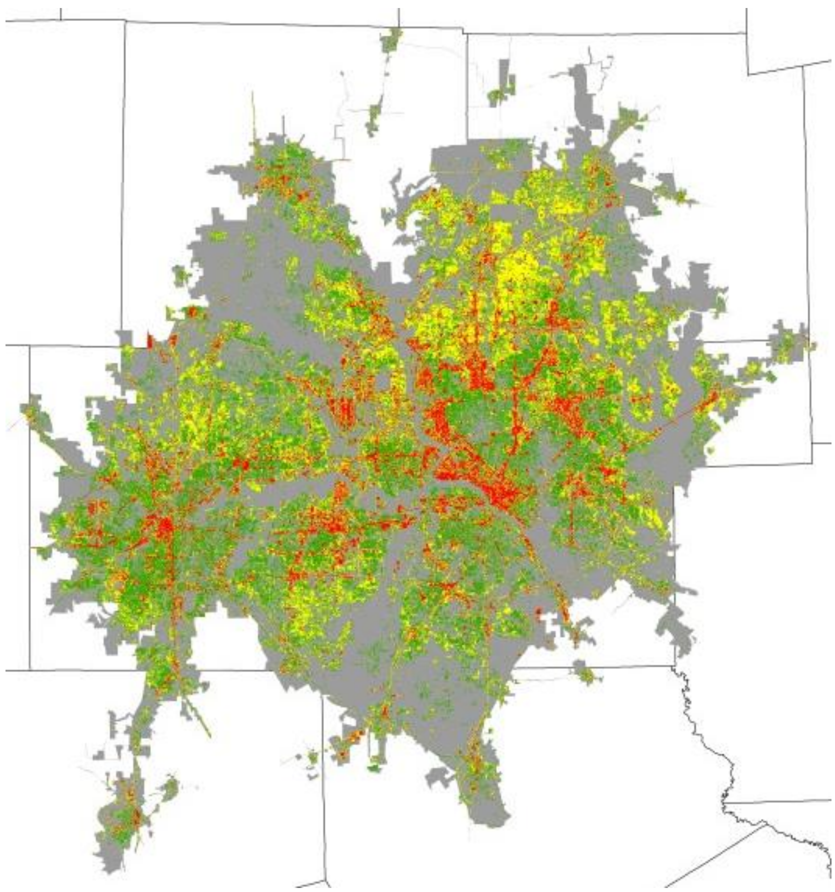

Figure 4.2: Dallas Metro Region

[12] National Land Cover Database 2011 (NLCD2011), Product Legend. Multi-Resolution Land Characteristics Consortium. http://www.mrlc.gov/nlcd11_leg.php

4.2.2 Site Selection

Estimates of the potential distributed solar generation within the 3 land use classes across the 4 metro regions were evaluated, resulting in a total of 12 DPV sites. Aerial imagery was analyzed to provide an indication of the intensity of development and approximate the energy density per unit land area. For each site, multiple 0.04-km^2 samples were evaluated (200-m by 200-m pixels).

First, the sample areas for each site were examined by aerial imagery to determine the percentage of each sample that is rooftop, and an average was calculated for each land use class. Next, an assumption was made for the percentage of rooftops that are optimally oriented for PV. Multi-level pitched rooftops were observed across much of the low and medium intensity developments (i.e., mostly small dwellings such as single family homes), and only one half of these rooftops was considered to be sloping optimally for PV (relatively south facing). High-intensity developments were found to have a higher fraction of the rooftops appropriately oriented for PV due to their mostly flat and continuous rooftop faces (e.g. large housing developments and commercial or industrial buildings). The percentage of the remaining optimal area that may actually be usable (due to chimneys, skylights, HVAC, azimuth, etc.) was then estimated. Finally, a plant density was assumed based on the types of systems likely to be installed in each land use class. The result was an energy density assumption for each land use class (Table 4.2). The density assumptions were applied to the available land area to obtain the maximum potential DPV capacity for each metro region (Table 4.3). No other exclusions were applied.

Table 4.2: Distributed PV Assumptions by Intensity of Development

Assumption	Low	Med	High
Buildings (% of land area)	20	26	35
Optimal (% of buildings)	50	50	90
Usable (% of optimal)	18.75	18.75	60
Plant density assumption (W/m^2)	45	45	50
Final density assumption (MW/km^2)	0.84	1.10	9.45

Table 4.3: Capacity (MW_{AC}) by Metro Region by Intensity of Development

Metro Region	Low	Med	High
Austin	261.67	309.60	927.34
Dallas	1,203.55	1,274.16	5,035.41
Houston	878.00	1,447.85	5,117.79
San Antonio	325.82	321.21	1,329.83

5. GENERATION PROFILES

5.1 Solar Irradiance Time Series Development

AWST developed a time series of hourly PV generation profiles covering a 19 year period from 1997-2015, for the selected theoretical utility-scale and DPV sites, as well as additional existing plants. Several of the existing sites also served as points for validation and adjustment. For each WRF grid cell associated with these locations, time series of the variables that impact module performance and power conversion were extracted, including global horizontal irradiance (GHI), direct normal irradiance (DNI), diffuse horizontal irradiance (DHI), temperature at 2 m above ground level, specific humidity at 2 m above ground level, wind speed at 10 m above ground level, rain, snow, and freezing rain.

Time series from 12 publicly-available, high quality solar surface stations with available GHI, DNI, and DHI measurements were used to validate and adjust the modeled irradiance time series. The frequency distribution of the modeled irradiance time series was adjusted to better reflect the distribution of observed values. This process adjusts both the means and the extremes of modeled irradiance data, and results in a more accurate representation of clear, partly cloudy, and cloudy days. The adjustment effectively eliminated the annual irradiance bias at all twelve validation stations, resulting in an average bias of -1.8 W/m^2, -1.1 W/m^2, and -14.3 W/m^2 for GHI, DHI, and DNI, respectively. (The root-mean-squared error (RMSE) after adjustment is 19.4 W/m^2, 5.4 W/m^2, and 51.4 W/m^2 for GHI, DHI, and DNI.)

5.2 Conversion to Power

The adjusted WRF irradiance and other meteorological variables served as input to AWST's power conversion software to synthesize solar PV generation profiles. Net PV profiles were synthesized for each of the hypothetical utility-scale and DPV sites described in Section 4 as well as at the location of several existing sites (six existing utility-scale plants, as well as one sample rooftop system in the city of Austin).

Hypothetical sites were modeled with the generic characteristics listed in Table 5.1. All utility-scale systems were assumed to be tilted to the mean latitude of the site and facing south. DPV systems were assumed to be tilted to 22.6 degrees (a common rooftop pitch in Texas) and were modeled using a variety of azimuths to capture real-world scenarios in which roofs may not be optimally oriented.

Existing sites were modeled with plant-specific parameters when known (Table 5.2). Unknown values were assumed to match the assumptions for the hypothetical sites. For some sites, only some module characteristics were known, so specific modules were assumed. When no module characteristics were known, a composite utility-scale module was used. Specifications for these modules are given in Table 5.3.

The composite module efficiency was increased 4% (to 20.7% and 20.2%) to reflect improved module technology at future PV installations for the hypothetical utility-scale and DPV sites, respectively.

Table 5.1: Characteristics of Hypothetical Sites Modeled

Plant Type	Tracking System	Tracking Type	Tilt (°)	Azimuth(s)	DC:AC ratio
Utility	Single	N-S	Latitude	0	1.3
Utility	Dual	NA	NA	0	1.25
DPV	Fixed	NA	22.6	+/-45, 0	1.25

Table 5.2: Characteristics of Existing Sites Modeled

Plant	Capacity (MW_{AC})	Tracking System	Tracking Type	Tilt	Azim	DC:AC ratio	Module Type
1	10.0	Single	N-S	Latitude*	0	1.30*	Utility Composite*
2	29.4	Single	N-S	Latitude*	0	1.30*	FirstSolar PD-5-401-03*
3	26.7	Single	N-S	Latitude*	0	1.17	Trina TSM-PA14*
4	160.0	Single	N-S	Latitude*	0	1.40	Canadian Solar CS6X-P
5	39.2	Dual	NA	NA	0	1.25*	Utility Composite*
6	37.6	Dual	NA	NA	0	1.22	Utility Composite*
Austin DPV	0.00624	Fixed	NA	20	0	1.25	Jinko JKM240M-60

* indicates assumed parameter

Table 5.3: Module Specifications

Module	Rated Capacity (W)	Efficiency (%)	Temperature Coefficient of Power (%)	Area (m^2)
Utility Composite	325	16.70	-0.41	1.94
Rooftop Composite	261	16.20	-0.42	1.63
FirstSolar PD-5-401-03	90	12.50	-0.25	0.72
Trina TSM-PA14	275	14.20	-0.45	1.94
Canadian Solar CS6X-P	315	16.94	-0.41	1.92

The power conversion process proceeded with the following steps:

- The number of PV modules necessary to reach a site's presumed rated capacity was calculated using its module's rated capacity. The PV area was then calculated by multiplying the number of modules by the composite module area. This area was then used in the power output calculations.
- Modeled irradiance was translated into plane-of-array values (irradiance incident on the tilted modules) using solar geometry for the direct components and the Perez method for the diffuse.[13] Single and dual-axis sites were modeled without tracking limits or backtracking capability.
- Gross power output was obtained by multiplying the PV area by the plane-of-array global irradiance and the appropriate module efficiency.
- The wind speed and temperature from the WRF-derived time series were used to calculate the PV module temperature. The PV temperature was used to calculate the reduction in module efficiency due to thermal factors. Utility-scale sites were assumed to have module cooling on the front and back face of the module, whereas the rooftop systems were assumed to have cooling on only one face.
- Static loss assumptions were applied to calculate each the net energy at each site. The static loss assumptions included in the net energy calculations are listed in Table 5.4. Losses due to temperature outside of inverter operating range are additional for utility-scale sites.

[13] R. Perez, P. Ineichen, R. Seals, J. Michalsky, and R. Stewart, 1990: Modeling daylight availability and irradiance components from direct and global irradiance. Solar Energy, 44, 271–289.

- Soiling loss assumptions were applied to calculate net energy. Soiling losses were varied based on precipitation, decreasing after significant rainfall and increasing after any snow accumulation.
- Row-to-row shading loss assumptions were applied to calculate net energy. Row-to-row shading losses were varied by time of day based on module spacing.[14] Neither horizon shading nor east-west shading were considered. Additionally, shading from rooftop obstructions was not considered for DPV.

In this way, 1-hour net solar PV profiles (1997-2015) were simulated for all sites. DPV profiles of varying azimuth were aggregated by site to account for sub-optimal orientation of some roofs. Results from the model were then compared with actual plant data in order to adjust loss assumptions, as described below.

Table 5.4: Fixed PV Loss Assumptions

Loss Source	%
Module Mismatch	1.25
Module Quality	1.00
Inverter Efficiency[15]	1.50
Availability of System and Substation	0.80
DC wiring	1.00
AC wiring	0.70
HVAC and Auxiliary Components	0.00
Transformer	1.00
Non-STC Operation (Irradiance)[16]	2.00
Degradation	0.00

5.3 Tuning Simulated Results to Observed Generation Data, and Validation

ERCOT provided historical generation profiles for five of the six existing utility-scale plants given in Table 5.2, as well as for one sample rooftop system in the city of Austin. These data were used to adjust the modeled generation time series so that the modeled net power of each site better reflected the observed values. These adjustments account for possible biases that may arise due to limitations in the simulated atmospheric data, plant and loss assumptions, or methodology. Adjustments were made separately for utility-scale single-axis, utility-scale dual-axis, and DPV sites.

Observed generation data from existing plants 1-3 were evaluated for use in adjusting the modeled generation time series at single-axis plants. Periods of curtailment, obvious changes in nameplate

[14] The modeled plants were designed to reduce row-to-row shading, thus this loss is expected to be less than 1%.

[15] Losses due to temperature outside of inverter operating range (-20°C to 50°C) are additional for utility-scale systems

[16] PV modules are rated under standard test conditions (STC) with a cell temperature of 25°C, irradiance of 1000 W/m^2, and air mass of 1.5. These conditions are rarely experienced in reality. The model adjusts the module efficiency for deviations from the standard temperature, and a static loss is applied to account for non-STC irradiance.

capacity,[17] or otherwise spurious data were removed from the observed data. Further evaluation of the plant 2 dataset showed deviation from the diurnal generation expected based on the assumed plant parameters (Table 5.2). Therefore, observed data from this plant were excluded from further analysis. After adjustments, the resulting single-axis modeled datasets exhibit a 2.8% aggregate bias relative to the observed mean generation. Results at existing plants 1 and 3 are shown in Figure 5.1 and Figure 5.2, respectively. A comparison of the aggregate modeled and observed generation at these plants is shown in Figure 5.3. Note that deviations from the observed generation values may be due to various modeling assumptions, namely DC:AC ratio, module type and tilt. Additionally, evaluation of individual days' profiles from single-axis sites show a midday "dip" in the observed net power during the wintertime months not reflected in the modeled data (not shown), possibly due to modules oriented with a tilt less than the site latitude (as was assumed).

The same process was used to adjust the modeled generation time series at the dual-axis plants for which historical generation data were available (existing plants 5 and 6). The loss assumptions were tuned to match the observed net power, and the resulting dual-axis modeled datasets exhibit a 1.3% aggregate bias relative to the observed mean generation. Results at plants 5 and 6 are shown in Figure 5.4 and Figure 5.5, respectively. A comparison of the aggregate modeled and observed generation at these plants is shown in Figure 5.6. As shown, the monthly and diurnal mean profiles of observed and modeled data match well, and better than the aggregate single-axis profile. This may also be indicative of a module tilt assumption as a contributing cause to the seasonal bias in production for the modeled single-axis sites (as the dual-axis tracking assumption nullifies any module tilt assumption).

The model predicts larger hourly ramps more frequently than observed for both single- and dual-axis profiles due to the modeled plants ramping from near zero to full capacity within the first hour of the day, and from full capacity to near zero within the last hour of the day. This may be due to the model not correctly accounting for increased shading with increased E-W module tilt at the beginning and end of the day. However, when only the hours of 10 AM to 3 PM were considered, the model was found to under-predict plant variability at individual plants, and the modeled plants were found to reach full AC capacity more often than observed (not shown). These discrepancies could be due to an underestimation of cloudiness in the model; however, the frequency distribution of clear and cloudy hours was adjusted to match observed values at reference sites during the process described in Section 5.1 (although seasonal biases remain). Discrepancies in daytime variability may also be due to an overestimate of the DC:AC ratio. A larger assumed DC:AC ratio results in a higher ratio of module to inverter capacity, which allows the net power to reach plant capacity despite losses being applied. When profiles for all existing plants were aggregated, the model predicts observed variability well midday (10 AM to 3 PM) as well as when all hours are considered (Figure 5.7). The remaining larger ramps in modeled data are likely due to a slight time shift in the modeled data, where the average modeled day begins slightly earlier and ramps more steeply than the observed plants (Figure 5.1 through Figure 5.6).

[17] Due to changes in installed capacity reflected in the observed data, plants 2-3 were modeled with capacity values different from those listed in Table 5.2 for adjustment and validation.

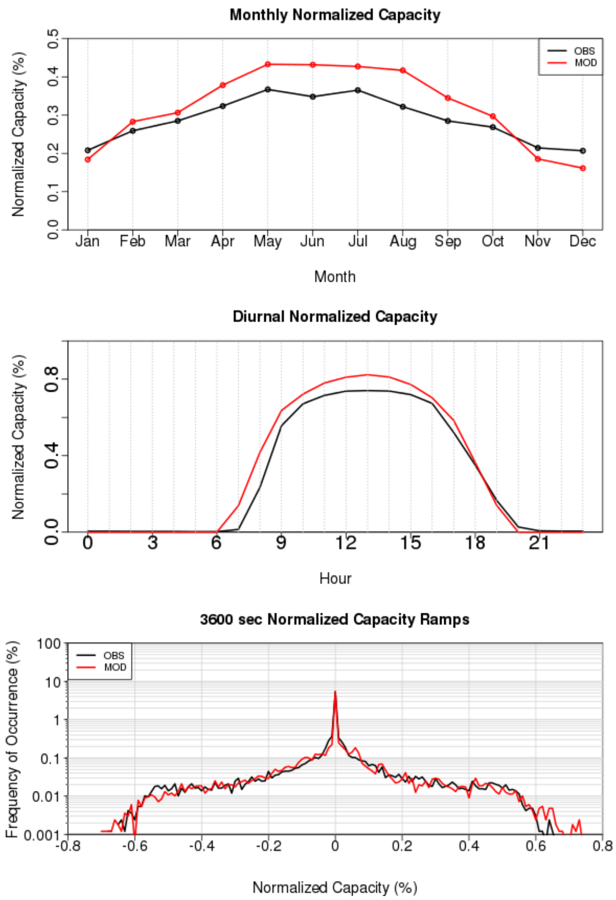

Figure 5.1: Observed (black) and Modeled (red) Generation Data Normalized by Plant Capacity at Existing Site 1

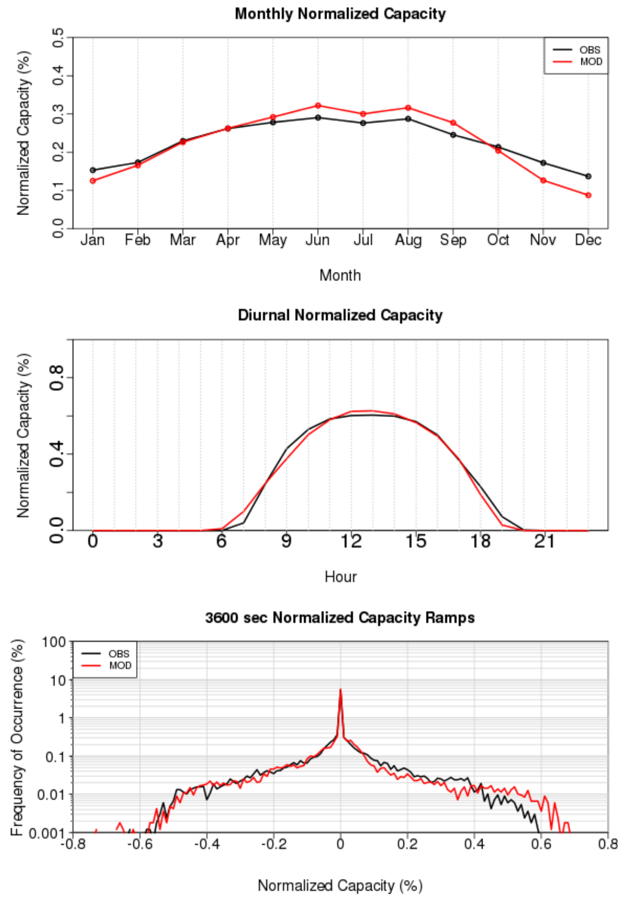

Figure 5.2: Observed (black) and Modeled (red) Generation Data Normalized by Plant Capacity at Existing Site 3

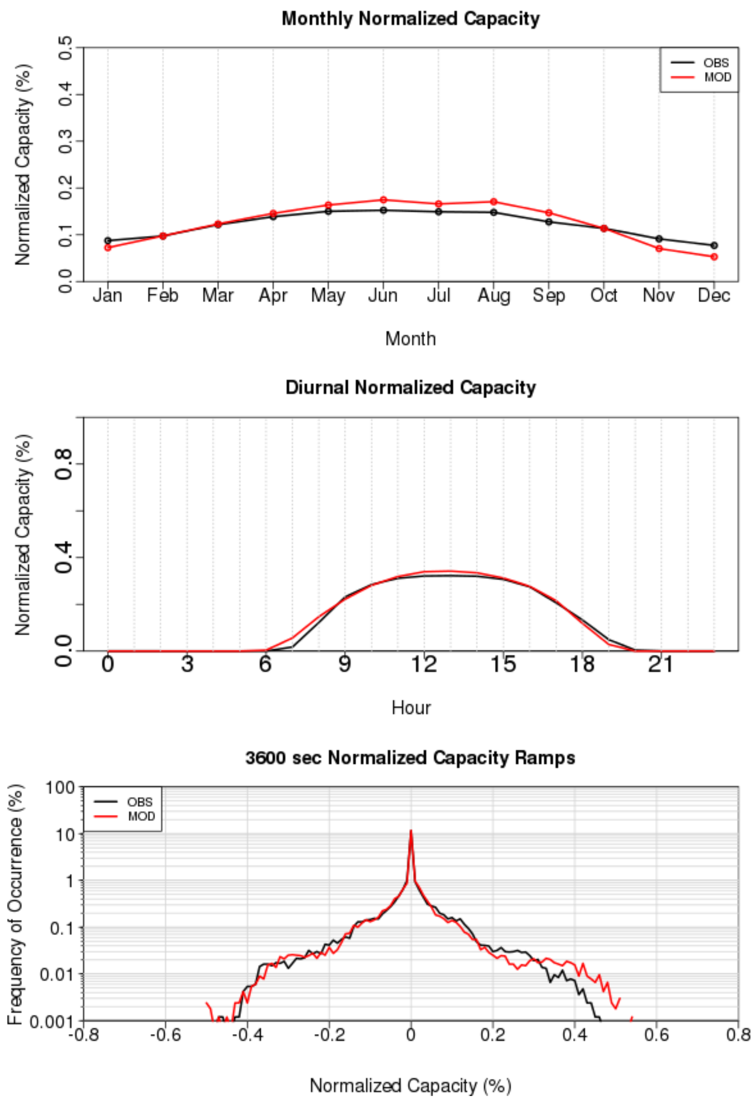

Figure 5.3: Aggregate Profiles of Observed (black) and Modeled (red) Generation Data Normalized by Aggregate Capacity for Existing Single-Axis Sites

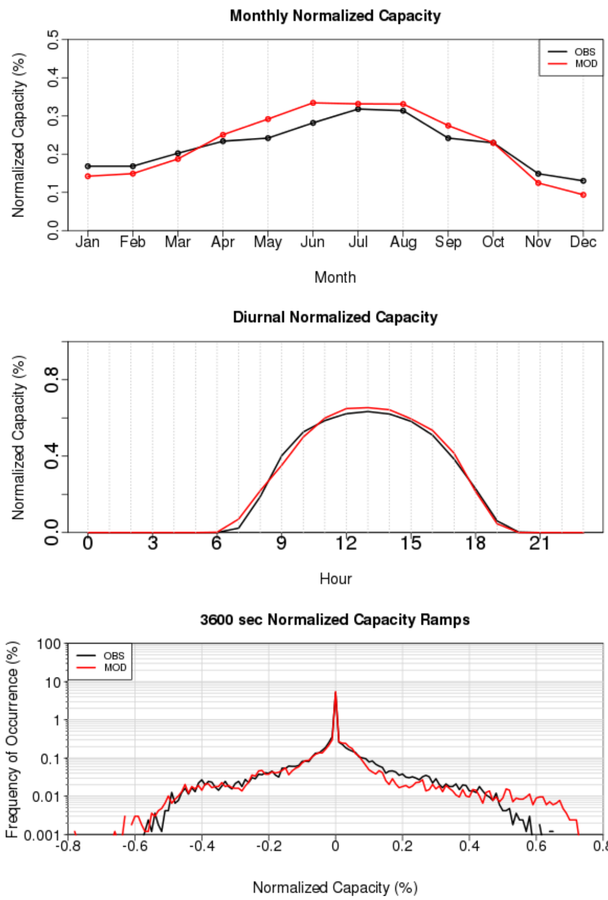

Figure 5.4: Observed (black) and Modeled (red) Generation Data Normalized by Plant Capacity at Existing Site 5

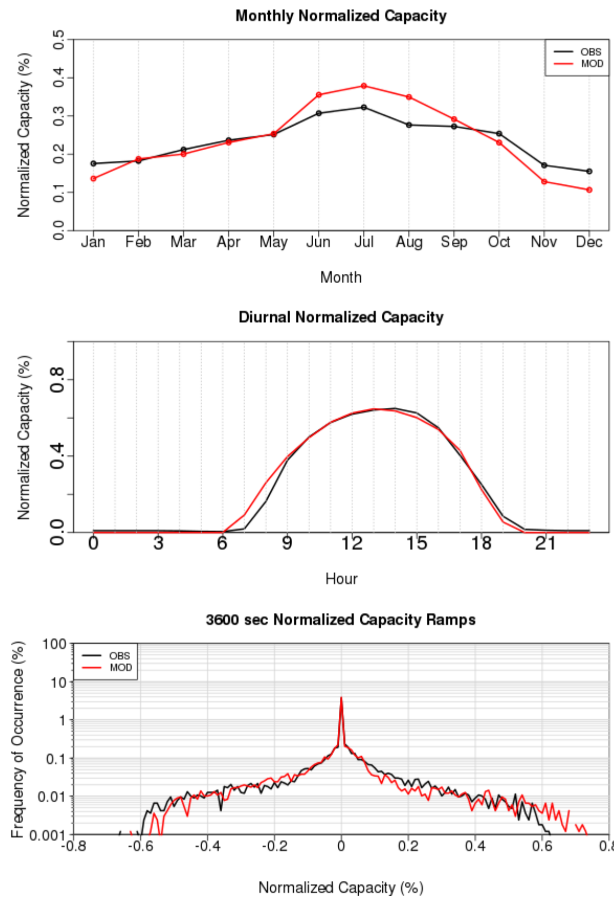

Figure 5.5: Observed (black) and Modeled (red) Generation Data Normalized by Plant Capacity at Existing Site 6

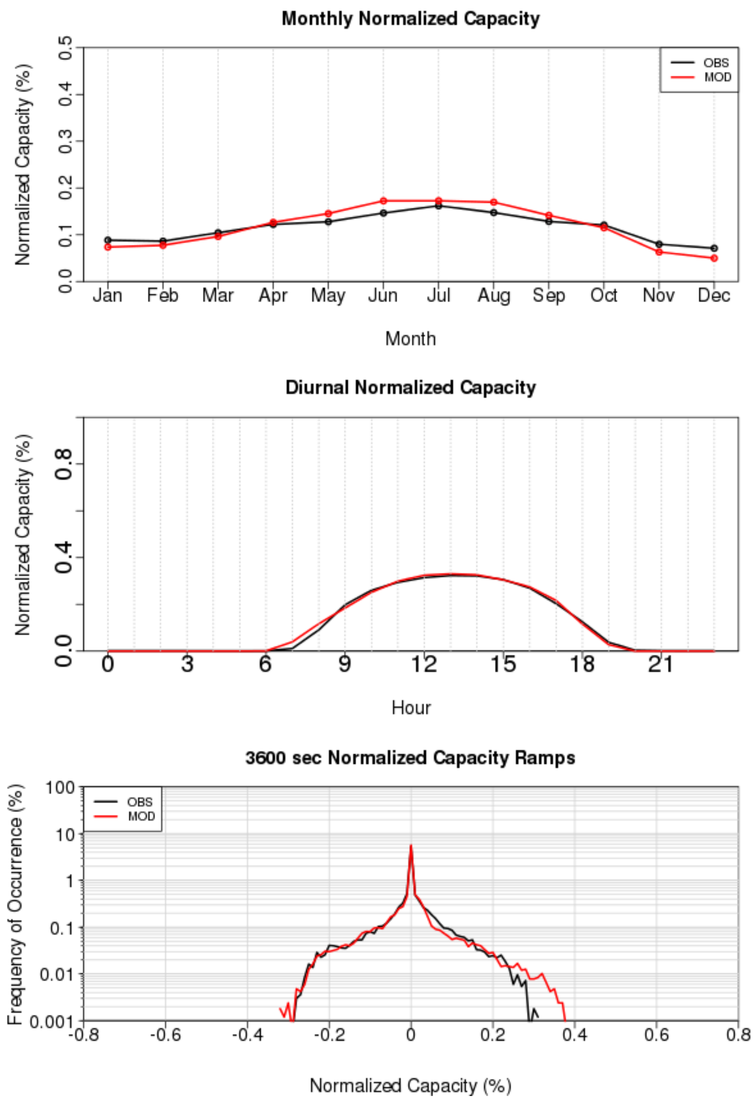

Figure 5.6: Aggregate Profiles of Observed (black) and Modeled (red) Generation Data Normalized by Aggregate Capacity for Existing Dual-Axis Sites

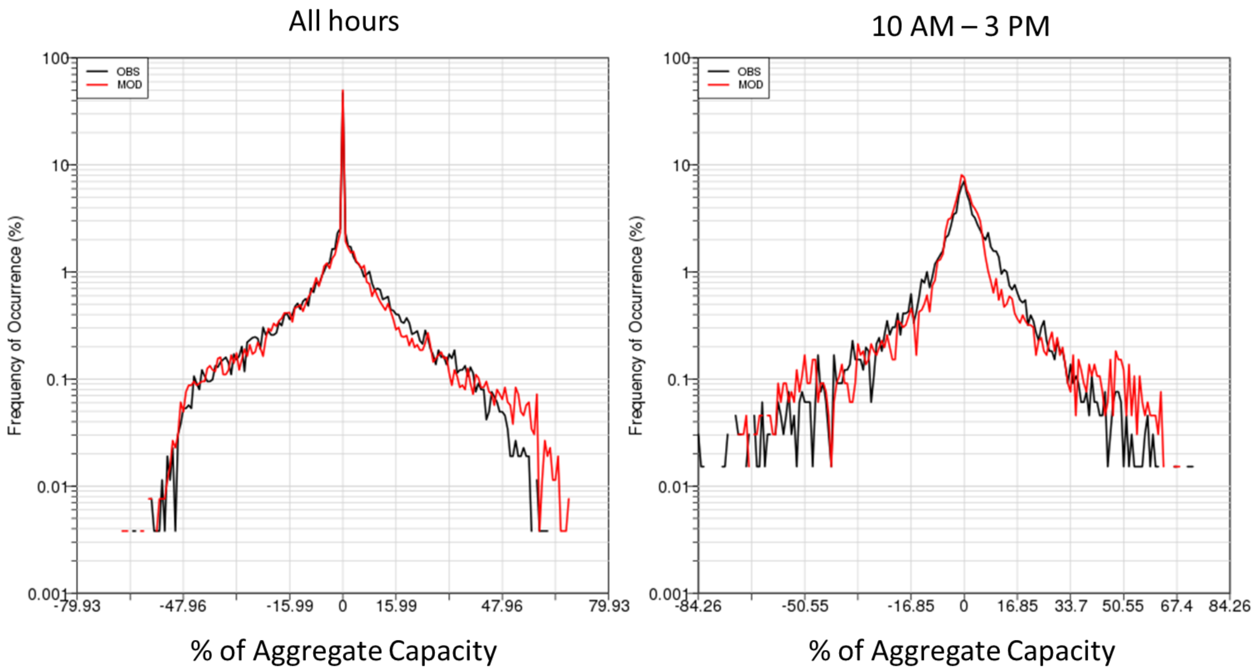

Figure 5.7: Frequency Distribution of Observed (black) and Modeled (red) Ramps Aggregated Over Existing Sites Modeled for All Hours (left) and 10 AM – 3 PM Only (right)

The tuning of the DPV time series proceeded as with the single- and dual-axis utility scale profiles. Data from the Austin DPV sample location was screened and used for adjustment. The final modeled dataset at this location exhibits a 1.4% annual bias.

5.4 Final Generation Profiles

Time series of generation profiles were developed for 125 hypothetical sites (single- and dual-axis), six existing utility-scale plants, and 12 DPV sites (representing three land use classes in four metro regions) for the years 1997-2015. The final single (dual) axis profiles have net capacity factor (NCF) values of 30.35 to 39.11% (30.75 to 39.51%), while the DPV profiles range from 21.79 to 21.92%. These profiles were evaluated for reasonableness and delivered in final form on November 04, 2016.

It was found that the assumed 4% increase in module efficiency accounts for approximately a 3% increase in NCF. The DPV profiles exhibit lower NCF values than utility-scale sites for a number of reasons. First, the DPV sites are located in eastern Texas where clouds are more prevalent than the west Texas utility-scale sites. Furthermore, the roof-mounted systems were modeled without tracking capability at a variety of azimuths, as opposed to the utility-scale sites modeled with single and dual axis tracking and oriented due south. Finally, the roof-mounted systems were subject to higher temperature losses because they experience wind-driven cooling only on one of their faces (as opposed to both faces for ground-mounted utility-scale modules).

Time series of irradiance data were compared from neighboring utility-scale sites, and although neighboring sites may exhibit overall similarities in generation statistics, variability appears in their hourly time series, as expected, when clouds pass over a region. For example, sites 4 and 66 located in Presidio County in western Texas have similar NCF values of 38.63% and 38.39% for single-axis tracking, respectively (39.01% and 38.77% for dual-axis). Power generation at these two sites is very similar on days with little cloud cover, but their profiles appear markedly different for days with increased cloud cover (Figure 5.8).

Comparison of the single- and dual-axis profiles shows similar overall capacity factor values (34.8% for single- and 35.2% for dual-axis). Mean diurnal profiles are also similar, although there is variation in hourly time series. In Figure 5.9, concurrent single- and dual-axis generation profiles for Site 4 are shown. Generation at the beginning and the end of the day is similar for these time series, with the largest difference seen during midday due to the single-axis sites tilted to latitude as opposed to the dual axis sites optimally tracking the sun's altitude.

These time series are similar in overall statistics because of the assumptions made and modeling limitations. The single-axis plants were modeled with modules tilted to the mean latitude of the site. Modeling these plants with a horizontal tilt would result in a greater difference between datasets. No limits were placed on the rotation of the single-axis trackers; i.e., the AWST power conversion software allows the modules to rotate a full 180 degrees to track the sun across the sky. In the process of tuning the model at existing plants, it was found that limiting this angle of rotation produced a less realistic diurnal profile compared to observed data. Also, the AWST software does not account for backtracking, where the modules rotate backwards to minimize the amount of shading from the adjacent modules to the west.

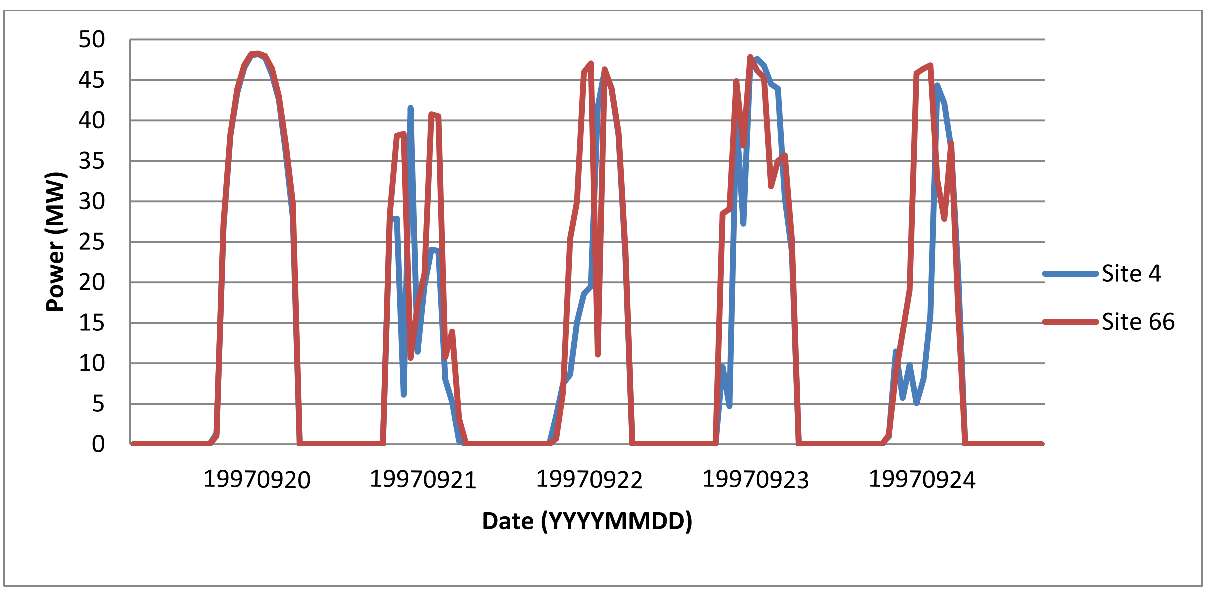

Figure 5.8: Generation Profiles Over 5 Days for Two Neighboring Sites

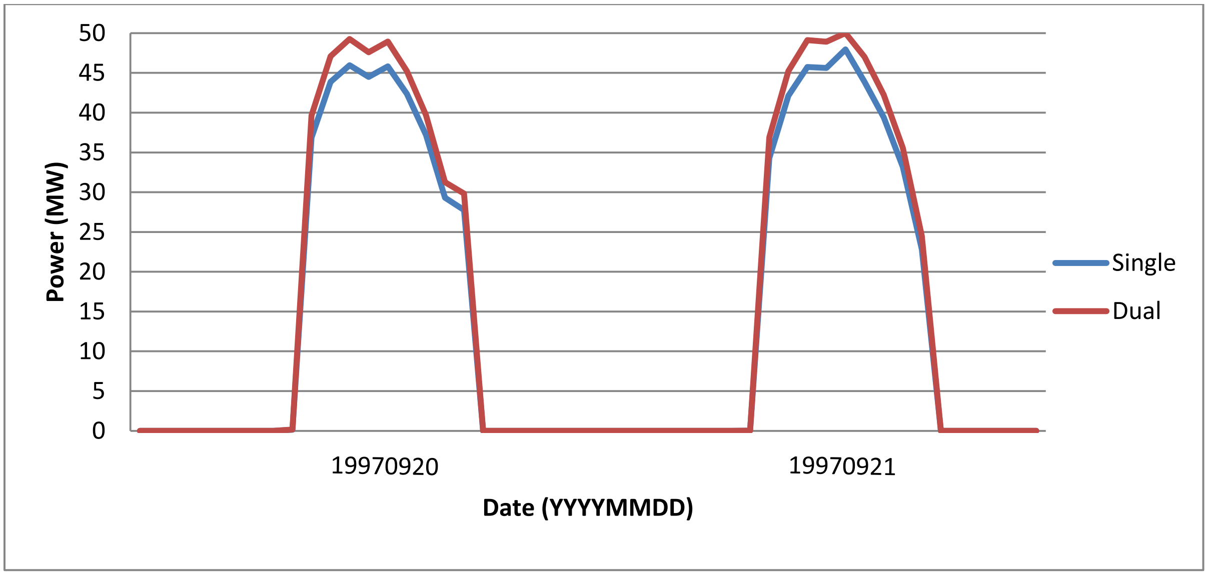

Figure 5.9: Concurrent Single- and Dual-Axis Profile Modeled for a Sample Site

6. DATASET USAGE

The solar data provided were developed specifically for use in large-scale regional planning studies for the purpose of observing the relative changes in solar PV generation across space and time. Of particular concern to ERCOT was the ability to realistically simulate the inter-hour, system-wide generation variability. Validation results show discrepancies exist when evaluating the single- or dual-axis plants separately. However, when results from all existing plants modeled are aggregated, these errors are diminished. Consequently, the time series provided are suggested to be used collectively for transmission and infrastructure planning, grid reliability studies, etc., as opposed to individual plant-level locational issue analyses.

The hypothetical sites modeled in this study were identified via a high-level identification of allowable land remaining after exclusions and additional assumptions were applied. Detailed analysis below 200-m resolution was not performed, and therefore some sites may not be commercially viable. Factors such as total area of contiguous land available to build, construct, and operate a solar PV plant with a reasonable cost of energy have not been considered, including significant factors such as proximity to existing roads and transmission. Additionally, policies and regulatory constraints have not been considered.

The profiles were modeled at a 9-km horizontal resolution. While this resolution captures much of the spatial variability in solar resource across the state of Texas, some details in the weather patterns may not be resolved at this scale. A more detailed analysis at a finer resolution is recommended for individual project sites that would better capture spatial and temporal variability that may exist between large and small plants.

Finally, it should be noted that modeled data is not a replacement for onsite measurements and should not be used as the only basis for investment decisions.

7. SUMMARY

A site selection process was completed for utility-scale and distributed solar PV sites within the state of Texas. For the screening of utility-scale sites, the process was designed to select representative 50 MW_{AC} single- and dual-axis sites distributed amongst the higher-irradiance counties in Texas. Each of these counties was represented by at least one site; two sites were modeled for the highest irradiance counties in West Texas. Distributed generation (rooftop solar) profiles were developed for residential and commercial or industrial areas for each of the following 4 metro areas: Austin, Dallas, Houston, and San Antonio. Density assumptions were applied to the total land area within the applicable land classes of each city, and total potential MW_{AC} capacity was estimated for these areas.

AWST utilized irradiance and other meteorological data simulated for the years 1997-2015 from 9-km WRF mesoscale weather model runs performed previously to support wind generation profiles for ERCOT. The modeled data were used to simulate power production profiles based on selected module technologies and tilt assumptions for existing and hypothetical utility-scale and distributed sites. The irradiance time series and power profiles were validated against observed data, and results confirm that these data reasonably represent the seasonal and diurnal patterns, ramping behavior, and power output of aggregate solar resources in the ERCOT region, despite modeling uncertainties. These data sets are suitable for use in system planning and solar resource integration studies.

APPENDIX

Table A.1: Utility-Scale Sites Listed by County (A-L)

County	Primary	Secondary
Andrews	745	
Armstrong	2804	
Bailey	1115	
Bexar	4433	
Borden	1403	
Brewster	30	211
Briscoe	2695	
Brown	3202	
Callahan	2864	
Cameron	2740	
Carson	2946	
Castro	1908	
Cochran	945	
Coke	2326	
Coleman	2925	
Concho	2168	
Cottle	3415	
Crane	577	686
Crockett	805	
Crosby	2101	
Culberson	176	352
Dallam	2785	
Dallas	5018	
Dawson	1136	
Deaf Smith	1348	
Dickens	2759	
Dimmit	1713	
Donley	3405	
Duval	2436	
Eastland	3116	
Ector	651	
Edwards	1720	
El Paso	225	277

County	Primary	Secondary
Fisher	2173	
Floyd	2560	
Frio	2688	
Gaines	831	
Garza	1980	
Gillespie	2437	
Glasscock	1008	
Hale	2062	
Hall	3399	
Harris	5718	
Hartley	2329	
Haskell	3061	
Hidalgo	1545	
Hockley	1238	
Howard	1217	
Hudspeth	100	163
Irion	1117	
Jeff Davis	105	197
Jim Hogg	1309	
Jones	2638	
Kent	2154	
Kerr	2405	
Kimble	2134	
King	3022	
Kinney	1923	
Knox	3443	
La Salle	2351	
Lamb	1336	
Loving	634	672
Lubbock	1992	
Lynn	1475	

Table A.2: Utility-Scale Sites Listed by County (M-Z)

County	Primary	Secondary
Martin	1047	
Mason	2346	
Maverick	1715	
McCulloch	2279	
McMullen	2870	
Menard	1999	
Midland	896	
Mills	3397	
Mitchell	1618	
Moore	3131	
Motley	3062	
Nolan	1957	
Oldham	2338	
Parmer	1233	
Pecos	136	419
Potter	3188	
Presidio	4	66
Randall	2512	
Reagan	906	
Real	3236	
Reeves	439	578
Runnels	2548	
San Saba	3005	
Schleicher	1487	
Scurry	2010	
Shackelford	3075	
Starr	1161	
Stephens	3284	
Sterling	1488	
Stonewall	2791	
Sutton	1633	
Swisher	2536	

County	Primary	Secondary
Taylor	2416	
Terrell	509	744
Terry	1162	
Throckmorton	3225	
Tom Green	1919	
Travis	5044	
Upton	647	
Uvalde	2723	
Val Verde	736	
Ward	555	622
Webb	1097	
Willacy	2916	
Winkler	699	704
Yoakum	903	
Zapata	1158	
Zavala	1914	